MCB Accepts, published online ahead of print on 19 March 2012
Mol. Cell. Biol. doi:10.1128/MCB.06726-11

The role of Ceroid Lipofuscinosis Neuronal protein-5 (CLN5) in endosomal sorting.

Aline Mamo[*1], Felix Jules[*1], Karine Dumaresq-Doiron[*], Santiago Costantino[*†] and Stephane Lefrancois[*∞‡]

1 These author contributed equally to this work

* Centre de Recherche de l'Hôpital Maisonneuve-Rosemont, Montréal, Canada H1T 2M4

∞ Département de Médecine, Université de Montréal, Montréal, Canada H3T 3J7

† Département d'Ophtalmologie et Institut de Génie Biomédical, Université de Montréal, Montréal, Canada H3T 1J4

‡ Corresponding author: Stephane Lefrancois, stephane.lefrancois@umontreal.ca

Running Title: CLN5 controls endosomal sorting

Word Count Materials and Methods:

Word Count Other Sections:

Abstract

Mutations in the gene encoding CLN5 are the cause of Finnish variant late infantile Neuronal Ceroid Lipofuscinosis (NCL), one of 10 genes (CLN1 - CLN9 and cathepsin D) whose germline mutations result in a group of recessive disorders of childhood. Although CLN5 localizes to the lysosomal compartment, its function remains unknown. We have uncovered an interaction between CLN5 and the lysosomal sorting receptor, sortilin. However, unlike prosaposin, CLN5 does not require sortilin to localize to the lysosomal compartment. We demonstrate that in CLN5-depleted HeLa cells, the lysosomal sorting receptors sortilin and CI-MPR are degraded in lysosomes due to a defect in retromer (an endosome-to-Golgi trafficking component) recruitment. Moreover, we also show that the retromer recruitment machinery is also affected by CLN5-depletion as we found less GTP-loaded Rab7, which is required to recruit retromer. Taken together, our results support a role for CLN5 in controlling the itinerary of the lysosomal sorting receptors by regulating retromer recruitment at the endosome.

Introduction

Neuronal Ceroid Lipofuscinosis (NCL) is a group of recessive disorders of childhood characterized by progressive vision loss, seizures, ataxia, deafness, mental retardation, and greatly reduced lifespan (18, 24). At the cellular level, NCL is characterized by an accumulation of autofluorescent lipopigments with morphological heterogeneity between various forms (12). Several forms of NCL have been identified based on age of onset, progression of disease, neurophysiological and histopathological findings. These disorders are the result of germline mutations in at least 10 genes (CLN1 - CLN9 and cathepsin D) (18), but the precise function of most of these proteins are still unknown, although most encode either soluble or transmembrane proteins localized to either the endoplasmic reticulum (ER) or endosomes/lysosomes.

CLN1 (also known as palmitoyl-protein thioesterase-1 (PPT1)) is a soluble lysosomal palmitoylthioesterase with no known endogenous substrates, but a deficiency in this enzyme causes infantile onset NCL (3). CLN3 is a transmembrane protein that has been shown to have palmitoyldesaturase activity (25) and may play a role in lysosomal acidification, organelle fusion, and apoptosis (28, 29). Mutations in the CLN3 gene cause juvenile NCL, more commonly known as Batten's disease. The exact function of CLN3 is still not fully elucidated, however it was recently proposed that it affects lysosomal trafficking and sorting in yeast and mammalian cells (9, 23). Moreover, ablation of CLN3 caused an accumulation of the lysosomal sorting receptor CI-MPR in the trans-Golgi network (TGN) (23) and these studies found a maturation defect of the soluble lysosomal protein cathepsin D, supporting a role for CLN3 in sorting to the lysosomal compartment. Although the function of CLN5 is unknown, germline mutations in the gene encoding this protein are implicated in Finnish variant late infantile NCL (33). In humans, the CLN5 gene maps to chromosome 13q22 and consists of 4 exons, spanning 13Kb of genomic DNA and encodes a protein of 407 amino acids. The predicted amino acid sequence of CLN5 shows no homology to previously reported proteins and although several studies suggested that CLN5 has at least one transmembrane domain (4, 33, 38), other studies report that it may be a soluble protein (16). Whereas transfection of COS-1 cells with CLN5 cDNA results in the synthesis of a highly glycosylated 60 kDa polypeptide, in cell-free translation assays 47, 44, 42 and 40 kDa polypeptides were produced due to usage of alternative initiator methionine (17). Finally, previous studies have shown that CLN5 interacts with CLN2 and CLN3 (38) and is localized to the endosomal/lysosomal compartment (17). However, the

mechanism cells use to sort CLN5 to lysosomes and the function of this protein remain unknown.

The trafficking of soluble luminal lysosomal cargo such as cathepsin D, CLN1, prosaposin and β-glucocerebrosidase are sorted by the cationic-dependent mannose 6-phosphate receptor (CD-MPR), the cationic-independent mannose 6-phosphate receptor (CI-MPR), sortilin and LIMP-II (7, 10, 20, 30). For anterograde traffic (Golgi-to-endosome), cargo binds to the receptors in the Golgi and is packaged into clathrin coated vesicles (5). When the receptor/cargo complex reaches the more acidic environment of the endosomes, the cargo dissociates from the receptor and the majority of the receptor is recycled back to the Golgi for another round of sorting while a small percentage is degraded in lysosomes (6). The efficient retrograde traffic (endosome-to-Golgi) of CI-MPR and sortilin requires the protein complex, retromer (1, 35). Mammalian retromer comprises 2 distinct subcomplexes: a dimer of a still undefined combination of sorting nexin 1 (SNX1), SNX2, SNX5 and SNX6 that can interact with the endosomal membrane via phosphatidylinositol 3-phosphate (PI3P) and a heterotrimer composed of vacuolar protein sorting 26 (Vps26), Vps29 and Vps35 that can bind the cytosolic tails of the lysosomal sorting receptors (2, 6).

A recent study found that CI-MPR was not implicated in the lysosomal localization of CLN5 (34). We tested the hypothesis that sortilin is involved in the sorting and trafficking of CLN5 to the lysosomal compartment. We report an interaction between CLN5 and sortilin, however, CLN5 is still properly localized in sortilin-depleted cells. Interestingly, in CLN5-depleted cells, we found that CI-MPR and sortilin are degraded in lysosomes due to the lack of retromer recruitment to endosomes. Taken together, we propose that CLN5 is part of an endosomal switch that determines whether the lysosomal sorting receptors are recycled back to the Golgi or degraded in lysosomes.

Materials and Methods

Antibodies and reagents

The following mouse monoclonal antibodies were used: anti-CD222 against CI-MPR, anti-myc 9E10, anti-HA, MMS-118P against GFP (all from Cedarlane Laboratories, Burlington, ON), anti-CD63, anti-SNX1 and Ab-5 against actin (both from BD Bioscience, Mississauga, ON). The

following polyclonal antibodies were used: anti-cathepsin D (Cedarlane Laboratories, Burlington, ON), anti-Lamp2 and anti-TGN46 (Sigma-Aldrich, Oakville, ON), anti-SNX3, anti-AP3, anti-RFP, anti-Vps26, anti-VPS35 and anti-prosaposin (all from Abcam, Cambridge, MA), anti-CLN5 and anti-CLN1 (both from Santa Cruz Biotechnology, Santa Cruz, CA). The cDNA for RFP-Rab5 and RFP-Rab7 were acquired from Addgene (Cambridge, MA). The HA-CLN5 construct was purchased from Genecopoeia (Germantown, MD). pGEX-RILP$_{220-299}$ was a generous gift from Dr. Aimee Edinger, (University of California, Irvine, CA). The cDNA for CLN1 and myc-CD63 was purchased from Origene (Rockville, MD). The dominant active Rab7 (RFP-Rab7Q67L) and the dominant negative Rab7 (RFP-Rab7T22N) were generated by site directed mutagenesis. The myc-Rab1a construct was a generous gift from Dr. Terry Hebert (McGill University, Montreal, QC).

Cell culture and immunofluorescence

Cells were maintained in DMEM supplemented with 10% fetal calf serum and antibiotics. Transfections were performed using 1µg of DNA per 2 cm plate with Lipofectamine Reagent supplemented with the Plus Reagent according to the manufacturer's instructions (Invitrogen, Burlington, ON). Stable cells lines were generated by the addition of 400 µg/ml of G418 for 2 weeks. Resistant clones were maintained under selective pressure by the addition of 200µg/ml of G418. Immunofluorescence was performed as previously described (11)

Co-immunoprecipitation, Cycloheximide chase and GST pull-down

These methods were previously described (19, 21).

RNA interference

The siRNA against CLN5 and CLN1 were purchased from Invitrogen and transfected using Oligofectamine (Invitrogen, Burlington, ON) according to the manufacturer's instructions. The siRNA against the 3'UTR of CLN5 was purchased from IDT DNA (Coralville, IA) and used according to the manufacturer's instructions. Cells were depleted of CLN5 and CLN1 using 100 nM of siRNA and grown for 48 hours before performing our assays. To deplete sortilin, HeLa cells were transfected with shSortilin using Lipofectamine Reagent according to the manufacturer's instructions (Invitrogen, Burlington, ON).

Quantification of immunofluorescence signals at the endosome

The endosomal compartment was assumed to be fluorescent puncta, most of them of subdiffraction-limit size. Widefield fluorescent microscopy images were taken using a 63x oil-immersion objective and appropriate dichroics to detect Alexa594, RFP or GFP. The exposure time of the camera was set in order to avoid saturation and maximize the intensity dynamic range, and was kept constant for the all acquired images. To accurately analyze the data in a non-biased way, an algorithm was custom programmed using Matlab (Mathworks, MA) which automatically detects puncta and computes their mean fluorescence in images composed of several cells. Fluorescent puncta were detected using linear band-pass filters that preserved objects of a size window and suppressed noise and large structures. These filters were applied by performing two 2-dimensional convolutions of the image matrix with a Gaussian and a boxcar kernel. Firstly the image was convolved with a Gaussian kernel of the characteristic length of the noise. This is considered a low-pass filter since only fluctuations longer than this given length are kept after this operation. Secondly, the image matrix was convolved with a boxcar kernel twice as big as the point spread function. This last operation is a low-pass filter for near-diffraction limit objects. Finally the subtraction of the boxcar image from the Gaussian images becomes a band-pass filter to choose elements bigger than noise up to twice the diffraction limit. In order to limit the puncta considered in the calculation to those inside cells, an intensity threshold was established using Otsu's method (27). The cytosolic fluorescence was enough to use this automatic thresholding procedure to assign foreground pixels to cells and background pixels to empty space. This coarse estimation of the foreground pixels was further refined and used as a mask to consider only puncta inside cells and discard signal arising from culture debris and nonspecific staining. The first refinement was to clean the mask by removing isolated pixels (1s surrounded by eight 0s). Next, a morphological erosion (13) was performed and holes inside the mask were filled. Finally, the area of each individual object in the mask was measured and all objects smaller than 50 times the biggest object (often several cells close together) were removed. Using the already filtered image multiplied by the cells mask, an algorithm that finds intensity local maxima was applied to detect the brightest pixels. Each of these intensity maxima was considered as the brightest location of a puncta and circles of 4 pixels in radius were established around the maxima. For each set of images the mean intensity of all these circles was calculated as a measure of protein expression level. The program opened all images one by one,

performed the band-pass filter, established a mask to delineate cells, found endosomes circles, computed their mean intensity, and calculated the average intensity for all endosomes in the full set of images.

Membrane Isolation Assay

This experiment was performed as previously described (15, 36)

Photoaffinity labelling

24 hours post-transfection, Hela cells were resuspended in 60 µL of labeling buffer (10 mM HEPES pH 7.4, 1 mM MgCl2, 0.1 mM β-mercaptoethanol) and passed eight times trough a 23G needle at room temperature. Guanosine 5'-triphosphate [γ] 4-azidoanilide 2',3'-biotin-long chain-hydrazone (Affinity Photoprobes, Lexington, KY) was then added to a final concentration of 0.1 µM. The samples were then incubated at room temperature for 10 min and were than subjected to UV irradiation (254 nm, 6 mW/cm2) with a mounted lamp for 5 min to cross-link the probe to proteins. Labeling buffer was then added to 750 µL and RFP-Rab7 and RFP-Rab5 were immunoprecipitated using a monoclonal RFP antibody. The labeling reaction was then detected by Western blot using streptavidin-HRP.

Results

CLN5 interacts with but is not trafficked by sortilin. Although it is well established that CLN5 localizes to the endosomal/lysosomal compartment (17), few studies have addressed its mechanism of trafficking. A recent study showed that CLN5 was properly localized in CI-MPR deficient fibroblasts (34), so we tested the hypothesis that CLN5 is a cargo of sortilin. Since soluble cargo must bind a lysosomal sorting receptor, we wanted to determine whether or not CLN5 was an interactive partner of sortilin. To test this, we co-expressed HA-CLN5 and sortilin-myc in HeLa cells and immunoprecipitated CLN5 with anti-HA antibody from HeLa cell lysate (Figure 1A). We observed a specific band corresponding to sortilin-myc in the presence of HA-CLN5 at pH 7 (Figure 1A, top left panels) which was absent in lysates not expressing HA-CLN5 even though sortilin-myc was expressed in both. Similarly, sortilin-myc was able to co-immunoprecipitate HA-CLN5 when we immunprecipitated with anti-myc antibody (data not shown) and our immunoprecipitation protocol using anti-HA antibody was clean as shown using

a coomasie stained gel (data not shown). Next, we further investigated this interaction to determine whether or not CLN5 is a cargo of sortilin. Earlier studies have established that lysosomal cargo such as prosaposin will co-precipitate with their receptors, in this case sortilin, when immunoprecipitation experiments are performed at pH 7, but these same interactions are lost when performed at a more acidic pH (39). We performed a co-immunoprecipitation of CLN5 and sortilin at pH 5 and found this interaction was pH independent (Figure 1A, top left panels) as CLN5 bound to sortilin at both neutral (Figure 1A, top left panels) and acidic pH (Figure 1A, top left panels) suggesting that CLN5 did not behave as a sortilin cargo protein. However, as predicted, the interaction between prosaposin and sortilin was weakened at pH 5 compared to pH 7 (Figure1A, top right panels) as prosaposin-myc could not efficiently co-immunoprecipitate sortilin-GFP at pH 5 but could at pH 7. The CLN5/sortilin interaction was specific as HA-CLN5 was not able to co-immunoprecipitate the lysosomal membrane protein myc-CD63 at either pH levels (Figure 1A, lower panels). To confirm that CLN5 is not a cargo of sortilin we tested if CLN5 was properly localized to the lysosomal compartment or not in sortilin-depleted cells. We transfected HeLa cells with (short hairpin) shSortilin to knockdown sortilin and obtained a 50% decrease in the absolute amount of sortilin following the knockdown (Figure 1B). An immunofluorescence assay performed on mock- (Figure 1C, D and E) and sortilin-depleted cells (Figure 1F, G and H) shows that CLN5 localization is not affected by the depletion of sortilin (Figure 1F, arrows). It was previously shown that prosaposin did not localize to lysosomes in sortilin-depleted cells (20), and as expected, the localization of prosaposin is perturbed in sortilin-depleted cells (Figure 1H) as shown by the lack of punctuate structures compared to mock-depleted cells (Figure 1E, arrows). Based on this data, we concluded that CLN5 is not a cargo of sortilin.

CLN5 is implicated in the trafficking of the lysosomal sorting receptors CI-MPR and sortilin. Since CLN5 is not a cargo of CI-MPR (34) or sortilin (our data), we examined the biological significance of the CLN5/sortilin interaction. We tested whether or not CLN5 plays a role in the steady-state localization of CI-MPR and sortilin by depleting CLN5 in HeLa cells using siRNA. We were able to efficiently deplete both CLN5 (Figure 2M) and CLN1 (Figure 2M) using a pool of 3 siRNAs as shown by Western blotting. We found that in CLN5-depleted cells (Figure 2J, K, L, J', K' and L'), the intensity of the immunofluorescence signal for endogenous CI-MPR (Figure 2K, star) and sortilin-myc (Figure 2K', star) were significantly

reduced compared to mock-treated cells (Figure 2H and H', arrows). However, the depletion of CLN1 (Figure 2D, E, F, D', E' and F'), a known CI-MPR cargo, did not have an effect on the localization or the intensity of CI-MPR (Figure 2E, arrow) or sortilin-myc (Figure 2E', arrow) compared to mock-depleted cells (Figure 2B and B', arrows). To verify that the Golgi was still intact in CLN5-depleted cells, we compared the immunofluorescence staining of the Golgi marker giantin in mock- and CLN5-depleted cells. We found no significant differences in giantin staining in mock-depleted (Figure 2N, red) compared to the CLN5-depleted (Figure 2O, red) cells suggesting that the Golgi was intact in CLN5-depleted cells. However, we found that TGN46 staining was fragmented in CLN5-depleted cells (Figure 2Q, red) compared to mock-depleted cells (Figure 2P, red) which was expected as similar phenotype was observed in retromer-depleted cells (35). In retromer-depleted cells, the immunofluorescence staining of CI-MPR is significantly reduced compared to mock-depleted cells and cycloheximide chase experiments show a degradation of the receptor in 6 hours (1, 31, 35). Since CLN5-depletion resulted in a similar immunofluorescence phenotype, we investigated whether the depletion of CLN5 would lead to the degradation of sortilin and CI-MPR with similar kinetics to retromer-depletion. To verify this, we performed a cycloheximide chase experiment and found that after incubation with cycloheximide for 6 hours, we found a significant reduction in the expression of CI-MPR (Figure 3A) and sortilin-myc (Figure 3A) in CLN5-depleted cells compared to mock- or CLN1-depleted cells which showed no significant degradation (Figure 3A). The depletion of CLN5 did not affect the total amount of the endosomal/lysosomal membrane protein CD63 (Figure 3A). Quantification of three separate experiments show a decrease of 46% and 59% respectively of CI-MPR and sortilin-myc in CLN5-depleted cells compared to mock-depleted while we found no significant changes in the expression of CD63 (Figure 3B). Significantly, the degradation kinetics in CLN5-depleted cells is similar as in retromer-depleted (1) or palmitoylation deficient cells, which is also required for retrograde trafficking of the lysosomal sorting receptors (21). Since the lysosomal sorting receptors were not being efficiently recycled to the Golgi and being degraded in CLN5-depleted cells, we would expect the mis-sorting of lysosomal cargo proteins such as cathepsin D or prosaposin. We found an increase in the amount of precursor and intermediate forms of cathepsin D in CLN5-depleted cells compare to mock-depleted cells (Figure 3C), which is consistent to previously published results from cells that had been either rab7- or retromer-depleted (32). Based on these experiments, we concluded

that the receptors in CLN5-depleted cells are not recycling back to the Golgi apparatus but are being degraded in lysosomes, suggesting that CLN5 plays a role in determining the itinerary of the lysosomal sorting receptors at the endosome.

CLN5 is required for the recruitment of Vps26 to endosomes. We next wanted to determine the mechanism that leads to the degradation of the lysosomal sorting receptors in CLN5-depleted cells. Since retromer-depletion leads to a similar phenotype as CLN5-depletion in terms of both stability and localization of CI-MPR and sortilin, we investigated the effect of CLN5-depletion on the recruitment of retromer to endosomal membranes. We found a significant decrease in the intensity of Vps26 immunofluorescence staining (Figure 4E, star) in CLN5-depleted (Figure 4D, E and F) compared to mock- (Figure 4A, B and C) or CLN1-depleted cells (Figure 4J, K and L). To rigorously quantify this observation, we developed an *ad hoc* algorithm to detect endosomes and quantify their fluorescence intensity. We obtained an unbiased image sample by randomly acquiring images from the total cell population. A representative immunofluorescence image is shown (Figure 4M, left panel) along with the mask that the software identifies as Vps26-positive structures (Figure 4M, right panel, red circles). This quantification revealed a 50% decrease in Vps26 immunofluorescence staining in the CLN5-depleted cell population (Figure 5A, black bar) compared to mock- (Figure 5A, white bar) or CLN1-depleted cells (Figure 5A, gray bar). This observed decrease in endosomal Vps26 intensity could indicate either degradation of the subunit (Vps26) or a block in recruitment of retromer to endosomal membranes. Thus, in order to differentiate between the two possibilities, we performed Western blotting to detect the absolute amount of the retromer subunit Vps26 and found no change in expression between mock-, CLN1- or CLN5-depleted cells (Figure 5B). To determine whether or not the depletion of CLN5 affected the intensity of immunofluorescence staining in endosome/lysosomes in general, we compared the immunofluorescence staining of CD63. The localization of this protein to the lysosomal compartment is retromer-independent. We found no significant difference in the immunofluorescence staining intensity of CD63 in mock- (Figure 5C, white bars) or CLN5-depleted cells (Figure 5C, black bars). It has previously been proposed that the Vps26, 29 and 35 trimer is recruited independently of the SNX dimer (composed of a combination of either SNX1, SNX, SNX5 and SNX6) (22). To gain further insight into the role of CLN5 in the recruitment of retromer to endosomal membranes, we investigated the effect of CLN5-depletion on the recruitment of SNX1 to endosomal membranes. Interestingly, we found no significant changes in

the amount of SNX1 recruited to endosomal membranes in CLN5-depleted cells (Figure 5D, black bar) compared to mock-depleted cells (Figure 5D, white bar) by immunofluorescence. To confirm our immunofluorescence data, we performed a membrane isolation experiment to determine the amount of Vps26, Vps35, AP3, SNX1 and SNX3 in the cytosol and on membranes in mock-, CLN5- and Rab7-depleted cells. We found less membrane bound and more cytosolic Vps26 and Vps35 in CLN5- and Rab7-depleted cells compared to mock-depleted cells (Figure 6A). However, we found no change in the distribution of SNX3, which is known to recruit retromer to endosomes to traffic the Wnt-binding protein Wntless (15) and blocks the efficient retrograde trafficking of the CD8-CI-MPR chimera (14), or SNX1 while AP3, an adaptor protein complex recruited to endosomes, seemed to be more cytosolic in Rab7-depleted cells while CLN5-depletion had no effect (Figure 6A). Lamp2 staining was used to identify the membrane fraction (Figure 6A). The quantification of 3 separate experiments shows the distribution of Vps26 and Vps35 in mock-, CLN5- and Rab7-depleted cells (Figure 6B). In mock-treated cells, 60% and 70% of Vps26 and Vps35 respectively are found in the membrane fractions (black bars) while in CLN5-depleted cells, the membrane fraction of Vps26 and Vps35 are reduced to 35% and 50% respectively while in Rab7-depleted cells the membrane association was 35% and 45% for Vps26 and Vps35 respectively. The changes in membrane association of retromer subunits obtained in the CLN5- and Rab7-depleted cells are comparable to those in previously published reports (15, 36) and supports a role for CLN5 in the recruitment of retromer to endosomal membranes.

In order to demonstrate that the effect seen on Vps26 recruitment is specific to CLN5-depletion and not an off-target effect, we adopted a rescue strategy in CLN5-depleted cells. For this, we knocked down endogenous CLN5 using a pool of siRNA directed against the 3'UTR of the designated gene and then reintroduced wild-type CLN5 to test for the rescued phenotype. Using this siRNA strategy, we obtained a 70% reduction in the amount of CLN5 (Figure 7A) which we could rescue with the expression of HA-CLN5 (Figure 7A). The knockdown of CLN5 against the 3'UTR resulted in the decreased recruitment of Vps26 (Figure 7B, black bar) as compared to mock treated cells (Figure 6B, white bar). Reintroducing wild-type HA-CLN5 in these CLN5-depleted cells rescued the recruitment of Vps26 (Figure 7B, grey bar). Taken together, these results point to a specific role for CLN5 in influencing the trafficking of lysosomal sorting receptors by controlling recruitment of retromer to endosomal membranes

CLN5 regulates the localization of Rab7. Next, we aimed to identify the molecular mechanisms underlying how CLN5 controls the recruitment of retromer to endosomes. Recently, it was shown that the activation of the small G proteins Rab5 and Rab7 are required for the recruitment the Vps26 subunit of retromer (32, 36). Since we obtained similar results by depleting cells of CLN5, we investigated whether CLN5 is implicated or not in Rab5 and Rab7 localization. We depleted cells of CLN5 and looked at the localization of RFP-Rab7 and RFP-Rab5. Our results show that in CLN5-depleted HeLa cells (Figure 8D, E and F), the intensity of RFP-Rab7 is lower compared to mock- (Figure 8B and H) or CLN1-depleted cells (Figure 8K). Quantification using our *ad hoc* algorithm showed a 40% decrease in the intensity of RFP-Rab7 at endosomes in CLN5-depleted cells (Figure 8M, black bar) compared to mock- (Figure 8M, white bar) or CLN1-depleted cells (Figure 8M, gray bar). Western blotting on whole cell lysate determined that the absolute amount of RFP-Rab7 in mock-, CLN1- and CLN5-depleted cells was similar (Figure 8N) suggesting that decrease in endosomal intensity was due to lack of recruitment and not degradation. We then compared the fluorescence intensity of RFP-Rab5 in mock- and CLN5-depleted cell and found a slight decrease (18%) in the intensity of RFP-Rab5 in CLN5-depleted cells (Figure 8O, black bar) compared to mock-depleted cells (Figure 8O, white bar). Consistent with our Rab7 data, we found no significant differences in the absolute amount of RFP-Rab5 as shown by Western blotting in either mock- or CLN5-depleted cells (Figure 8P). We next tested if CLN5 was in a protein complex with Rab5 and/or Rab7 by co-transfecting HeLa cells with HA-CLN5 and either myc-Rab1a, RFP-Rab5 or RFP-Rab7. Following an immunoprecipitation with anti-HA or anti-RFP antibodies, we found an interaction between HA-CLN5 and RFP-Rab5 and RFP-Rab7 (Figure 9A) but not with myc-Rab1a (Figure 9A). This suggested that CLN5 may act as a scaffold for the site of recruitment of Rab7 and subsequently retromer onto endosomal membranes.

CLN5 is required to activate Rab7. We next tried to determine whether CLN5 was an effector of activated Rab7 or if CLN5 was required to activate Rab7. We tested if dominant active Rab7 (RFP-Rab7Q67L) could interact more strongly with CLN5 than wild-type Rab7, suggesting it would be an effector like RILP (8), rubicon (37) or retromer (32). Following an immunoprecipitation with anti-HA antibody, we found that both wild-type Rab7 and dominant active Rab7 (Rab7Q67L) interacted with CLN5 (Figure 9B). Moreover, we also found an interaction between dominant negative Rab7 (RFP-Rab7T22N) and CLN5 (Figure 9B)

suggesting that CLN5 may be part of the Rab7 activation machinery and not an effector. Next, we compared the cells' ability to GTP load Rab5 and Rab7 in the presence or absence of CLN5 by measuring the amount of a cross-linkable GTP analogue incorporated into these Rab proteins. We found that, compared to mock-depleted cells, CLN5-depleted cells had significantly less GTP-loaded Rab7 (Figure 9C), while the amount of GTP loaded Rab5 was not significantly different (Figure 9C). Quantification of the GTP-loading experiments showed that in CLN5-depleted cells, Rab7 loading was reduced by 76% (Figure 9D, black bar) compared to mock depleted cells (Figure 9D, white bar) while the amount of GTP loaded Rab5 was not changed in mock- (Figure 9E, white bar) compared to CLN5-depleted cells (Figure 9E, black bar). In support of this data, Rab7 binding to Rab-interacting lysosomal protein (RILP), a known Rab7 effector (8), in a GST pull-down assay was less efficient in cells depleted of CLN5 compared to mock- or CLN1-depleted cells (Figure 9F). Taken together, these results show that CLN5 is required to recruit and activate Rab7 to subsequently recruit retromer to endosomal membranes.

Discussion

Several conclusions can be drawn from the data presented in this work. First, CLN5 interacts with sortilin. However this interaction is not required to traffic CLN5 to the lysosomal compartment but rather it enables the lysosomal sorting receptors (CI-MPR and sortilin) to recycle back to the Golgi from endosomes preventing their degradation. Secondly, to enable retrograde trafficking of the lysosomal sorting receptors, CLN5 is implicated in the recruitment of retromer to endosomes by regulating the localization and activation of Rab7, which has previously been shown to be implicated in retromer recruitment (32, 36). While it was known that CLN5 is localized to the endosomal/lysosomal compartment, its function and mechanism of trafficking have not been elucidated. Since a previous report found that CI-MPR was not implicated in the trafficking of CLN5 (34), we tested if sortilin was a trafficking receptor for CLN5. We found that CLN5 binds sortilin, however, CLN5 can interact with sortilin at a more acidic pH that usually inhibits cargo/receptor interactions such as prosaposin binding to sortilin. This suggested that the CLN5/sortilin interaction may not be required for the trafficking of CLN5 to the lysosomal compartment and in support of this, depletion of sortilin by shRNA had no effect on the cellular localization of CLN5, although it did prevent the proper localization of a known cargo, prosaposin, as was previously shown (20). Since neither CI-MPR nor sortilin seem

to be implicated in the trafficking of CLN5, it is possible that LIMP-II is required, as it was recently shown that this protein can act as the sorting receptor for β-glucocerebrosidase (30). Moreover, since CLN5 is a potential transmembrane protein, it is therefore possible that CLN5 can interact directly with cytosolic trafficking components to form its own trafficking vesicles like other lysosome integral membrane proteins such as CD63 and Lamp2. More work will be required to elucidate this sorting and trafficking mechanism.

To elucidate the biological significance of the CLN5 interaction with lysosomal sorting receptors, we used siRNA to deplete CLN5 in HeLa cells. In CLN5-depleted cells, we found that the retrograde trafficking of both sortilin and CI-MPR to the Golgi compartment was impeded which led to their degradation. Interestingly, CI-MPR and sortilin are degraded with similar kinetics in both CLN5- and retromer-depleted cells. Based on this, we tested the effect of CLN5-depletion on the recruitment of retromer to endosomes. Compared to mock- and CLN1-depleted cells, the recruitment of the Vps portion of retromer to endosomes is significantly reduced in CLN5-depleted cells as shown by a decrease in Vps26 localization to endosomal membranes by immunofluorescence and Vps26 and Vps35 by membrane isolation.

The recruitment of retromer to endosomal membranes is a tightly regulated process that requires the small G proteins Rab5 and Rab7 (32, 36). Our results show a significant reduction in the amount of Rab7 and a slight reduction in the amount of Rab5 found on endosomal membranes in CLN5-depleted cells. Interestingly, we also found that the activation of Rab7 was significantly impaired but found no changes in the activation of Rab5. A recent paper demonstrated that the Mon1-Ccz1 complex is a Rab GEF for the yeast homologue of Rab7 (26). It is possible that CLN5 could recruit this GEF to localize and/or activate Rab7. The molecular details of this event need to be further elucidated. If CLN5 is a transmembrane domain protein, it could be possible that CLN5 could interact directly with Mon1 and/or Rab7. Alternatively, the interaction could be indirect and mediated via CLN3, a known interactive partner of CLN5. Further work will be required to determine this.

Taken together, our results support a role for CLN5 in the retrograde trafficking of the lysosomal sorting receptors in mammalian cells. We propose, that upon arrival in the more acidic environment of the endosome (Figure 10, step 1), cargo dissociates from the lysosomal sorting receptors and is replaced by CLN5 (Figure 10, step 2). This provides a signal and/or scaffold to

recruit and activate Rab7 (Figure 10, step 2) followed by the recruitment of retromer (Figure 8, step 3). This then enables the receptor to traffic to the Golgi for another round of sorting and trafficking. In conclusion, results presented in this study are consistent with a new model suggesting that CLN5 acts as an endosomal switch allowing lysosomal sorting receptors to recycle back to the Golgi for another round of vesicular trafficking and cargo sorting.

Acknowledgments

The authors wish to thank Dr. Peter J. McCormick (University of Barcelona) and Christine L. Lavoie (University of Sherbrooke) for critical reading of this manuscript and for helpful discussions. This work was funded by grants from SickKids Foundation (XG08-027) and CIHR (Operating Grant MOP-102754) to S.L. and NSERC and FQRNT to S.C. S.L and S.C. are recipients of a salary award from Fonds de la recherche en santé du Quebec. A.M. is a recipient of a Nephrology research fellowship from the Fondation de l'Hôpital Maisonneuve-Rosemont.

References

1. **Arighi, C. N., L. M. Hartnell, R. C. Aguilar, C. R. Haft, and J. S. Bonifacino.** 2004. Role of the mammalian retromer in sorting of the cation-independent mannose 6-phosphate receptor. J Cell Biol **165:**123-133.
2. **Attar, N., and P. J. Cullen.** 2009. The retromer complex. Adv Enzyme Regul.
3. **Bellizzi, J. J., 3rd, J. Widom, C. Kemp, J. Y. Lu, A. K. Das, S. L. Hofmann, and J. Clardy.** 2000. The crystal structure of palmitoyl protein thioesterase 1 and the molecular basis of infantile neuronal ceroid lipofuscinosis. Proc Natl Acad Sci U S A **97:**4573-4578.
4. **Bessa, C., C. A. Teixeira, M. Mangas, A. Dias, M. C. Sa Miranda, A. Guimaraes, J. C. Ferreira, N. Canas, P. Cabral, and M. G. Ribeiro.** 2006. Two novel CLN5 mutations in a Portuguese patient with vLINCL: insights into molecular mechanisms of CLN5 deficiency. Mol Genet Metab **89:**245-253.
5. **Bonifacino, J. S., and J. Lippincott-Schwartz.** 2003. Coat proteins: shaping membrane transport. Nat Rev Mol Cell Biol **4:**409-414.
6. **Bonifacino, J. S., and R. Rojas.** 2006. Retrograde transport from endosomes to the trans-Golgi network. Nat Rev Mol Cell Biol **7:**568-579.
7. **Bonifacino, J. S., and L. M. Traub.** 2003. Signals for sorting of transmembrane proteins to endosomes and lysosomes. Annu Rev Biochem **72:**395-447.
8. **Cantalupo, G., P. Alifano, V. Roberti, C. B. Bruni, and C. Bucci.** 2001. Rab-interacting lysosomal protein (RILP): the Rab7 effector required for transport to lysosomes. EMBO J **20:**683-693.
9. **Codlin, S., and S. E. Mole.** 2009. S. pombe btn1, the orthologue of the Batten disease gene CLN3, is required for vacuole protein sorting of Cpy1p and Golgi exit of Vps10p. J Cell Sci **122:**1163-1173.
10. **Dahms, N. M., P. Lobel, and S. Kornfeld.** 1989. Mannose 6-phosphate receptors and lysosomal enzyme targeting. J Biol Chem **264:**12115-12118.

11. **Dumaresq-Doiron, K., M. F. Savard, S. Akam, S. Costantino, and S. Lefrancois.** 2010. The phosphatidylinositol 4-kinase PI4KIIIalpha is required for the recruitment of GBF1 to Golgi membranes. J Cell Sci **123:**2273-2280.
12. **Goebel, H. H., and K. E. Wisniewski.** 2004. Current state of clinical and morphological features in human NCL. Brain Pathol **14:**61-69.
13. **Gonzalez, R. C., R. E. Woods, and S. L. Eddins.** 2004. Digital Image processing using MATLAB. Pearson Prentice Hall, Upper Saddle River, N. J.
14. **Harbour, M. E., S. Y. Breusegem, R. Antrobus, C. Freeman, E. Reid, and M. N. Seaman.** 2010. The cargo-selective retromer complex is a recruiting hub for protein complexes that regulate endosomal tubule dynamics. J Cell Sci **123:**3703-3717.
15. **Harterink, M., F. Port, M. J. Lorenowicz, I. J. McGough, M. Silhankova, M. C. Betist, J. R. van Weering, R. G. van Heesbeen, T. C. Middelkoop, K. Basler, P. J. Cullen, and H. C. Korswagen.** 2011. A SNX3-dependent retromer pathway mediates retrograde transport of the Wnt sorting receptor Wntless and is required for Wnt secretion. Nat Cell Biol **13:**914-923.
16. **Holmberg, V., A. Jalanko, J. Isosomppi, A. L. Fabritius, L. Peltonen, and O. Kopra.** 2004. The mouse ortholog of the neuronal ceroid lipofuscinosis CLN5 gene encodes a soluble lysosomal glycoprotein expressed in the developing brain. Neurobiol Dis **16:**29-40.
17. **Isosomppi, J., J. Vesa, A. Jalanko, and L. Peltonen.** 2002. Lysosomal localization of the neuronal ceroid lipofuscinosis CLN5 protein. Hum Mol Genet **11:**885-891.
18. **Jalanko, A., and T. Braulke.** 2009. Neuronal ceroid lipofuscinoses. Biochim Biophys Acta **1793:**697-709.
19. **Lefrancois, S., K. Janvier, M. Boehm, C. E. Ooi, and J. S. Bonifacino.** 2004. An ear-core interaction regulates the recruitment of the AP-3 complex to membranes. Dev Cell **7:**619-625.
20. **Lefrancois, S., J. Zeng, A. J. Hassan, M. Canuel, and C. R. Morales.** 2003. The lysosomal trafficking of sphingolipid activator proteins (SAPs) is mediated by sortilin. Embo J **22:**6430-6437.
21. **McCormick, P. J., K. Dumaresq-Doiron, A. S. Pluviose, V. Pichette, G. Tosato, and S. Lefrancois.** 2008. Palmitoylation controls recycling in lysosomal sorting and trafficking. Traffic **9:**1984-1997.
22. **McGough, I. J., and P. J. Cullen.** 2011. Recent advances in retromer biology. Traffic **12:**963-971.
23. **Metcalf, D. J., A. A. Calvi, M. Seaman, H. M. Mitchison, and D. F. Cutler.** 2008. Loss of the Batten disease gene CLN3 prevents exit from the TGN of the mannose 6-phosphate receptor. Traffic **9:**1905-1914.
24. **Mole, S. E., R. E. Williams, and H. H. Goebel.** 2005. Correlations between genotype, ultrastructural morphology and clinical phenotype in the neuronal ceroid lipofuscinoses. Neurogenetics **6:**107-126.
25. **Narayan, S. B., D. Rakheja, L. Tan, J. V. Pastor, and M. J. Bennett.** 2006. CLN3P, the Batten's disease protein, is a novel palmitoyl-protein Delta-9 desaturase. Ann Neurol **60:**570-577.
26. **Nordmann, M., M. Cabrera, A. Perz, C. Brocker, C. Ostrowicz, S. Engelbrecht-Vandre, and C. Ungermann.** 2010. The Mon1-Ccz1 complex is the GEF of the late endosomal Rab7 homolog Ypt7. Curr Biol **20:**1654-1659.
27. **Otsu, N.** 1979. Threshold Selection Method from Gray-Level Histograms. Ieee Transactions on Systems Man and Cybernetics **9:**62-66.
28. **Phillips, S. N., J. W. Benedict, J. M. Weimer, and D. A. Pearce.** 2005. CLN3, the protein associated with batten disease: structure, function and localization. J Neurosci Res **79:**573-583.
29. **Ramirez-Montealegre, D., and D. A. Pearce.** 2005. Defective lysosomal arginine transport in juvenile Batten disease. Hum Mol Genet **14:**3759-3773.
30. **Reczek, D., M. Schwake, J. Schroder, H. Hughes, J. Blanz, X. Jin, W. Brondyk, S. Van Patten, T. Edmunds, and P. Saftig.** 2007. LIMP-2 is a receptor for lysosomal mannose-6-phosphate-independent targeting of beta-glucocerebrosidase. Cell **131:**770-783.

31. **Rojas, R., S. Kametaka, C. R. Haft, and J. S. Bonifacino.** 2007. Interchangeable but essential functions of SNX1 and SNX2 in the association of retromer with endosomes and the trafficking of mannose 6-phosphate receptors. Mol Cell Biol **27:**1112-1124.
32. **Rojas, R., T. van Vlijmen, G. A. Mardones, Y. Prabhu, A. L. Rojas, S. Mohammed, A. J. Heck, G. Raposo, P. van der Sluijs, and J. S. Bonifacino.** 2008. Regulation of retromer recruitment to endosomes by sequential action of Rab5 and Rab7. J Cell Biol **183:**513-526.
33. **Savukoski, M., T. Klockars, V. Holmberg, P. Santavuori, E. S. Lander, and L. Peltonen.** 1998. CLN5, a novel gene encoding a putative transmembrane protein mutated in Finnish variant late infantile neuronal ceroid lipofuscinosis. Nat Genet **19:**286-288.
34. **Schmiedt, M. L., C. Bessa, C. Heine, M. G. Ribeiro, A. Jalanko, and A. Kyttala.** 2010. The neuronal ceroid lipofuscinosis protein CLN5: new insights into cellular maturation, transport, and consequences of mutations. Hum Mutat **31:**356-365.
35. **Seaman, M. N.** 2004. Cargo-selective endosomal sorting for retrieval to the Golgi requires retromer. J Cell Biol **165:**111-122.
36. **Seaman, M. N., M. E. Harbour, D. Tattersall, E. Read, and N. Bright.** 2009. Membrane recruitment of the cargo-selective retromer subcomplex is catalysed by the small GTPase Rab7 and inhibited by the Rab-GAP TBC1D5. J Cell Sci **122:**2371-2382.
37. **Sun, Q., W. Westphal, K. N. Wong, I. Tan, and Q. Zhong.** 2010. Rubicon controls endosome maturation as a Rab7 effector. Proc Natl Acad Sci U S A **107:**19338-19343.
38. **Vesa, J., M. H. Chin, K. Oelgeschlager, J. Isosomppi, E. C. DellAngelica, A. Jalanko, and L. Peltonen.** 2002. Neuronal ceroid lipofuscinoses are connected at molecular level: interaction of CLN5 protein with CLN2 and CLN3. Mol Biol Cell **13:**2410-2420.
39. **Yuan, L., and C. R. Morales.** 2009. A Stretch of 17 Amino Acids in the Prosaposin C-terminus Is Critical for Its Binding to Sortilin and Targeting to Lysosomes. J Histochem Cytochem.

Figure Legends

Figure 1. CLN5 interacts with the lysosomal sorting receptors. (A) HeLa cells were transfected with sortilin-myc, myc-CD63, prosaposin-myc (psap-myc), sortilin-GFP and HA-CLN5 as indicated. Whole cell lysates were immunoprecipitated (IP) with anti-HA or anti-myc antibodies at the pH shown and Western blotted (Wb) with anti-myc, anti-HA or anti-GFP antibody. The amount of sortilin-myc, myc-CD63 or sortilin-GFP pre-immunoprecipitation (Pre-IP) is shown and represents 10% of the input. (B) HeLa cells transfected with sortilin-myc were either mock- or sortilin-depleted with a short-hairpin construct (shSortilin). Whole cell lysates were run on 12% acrylamide gels and Western blotted (Wb) with anti-myc and anti-actin antibodies. HeLa cells expressing sortilin-myc were mock transfected (C, D and E) or transfected with shSortilin (F, G and H) to deplete sortilin. Cells were fixed in 4% paraformaldehyde and immunostained with anti-CLN5 antibody (C and F, green), anti-myc antibody (D and G, green) or anti-prosaposin (PSAP) antibody (E and H, red). Arrows indicate the normal localization of

CLN5 (C and F), sortilin-myc (D) or PSAP (E). Stars indicate nuclear background staining for anti-prosaposin antibody (E and H). Scale bar = 10 µm.

Figure 2. CLN5 is required for the localization of CI-MPR and sortilin. HeLa cells were mock- (A - C, A' - C', G - I and G' - I'), CLN1- (D - F and D' - F') or CLN5-depleted (J - L and J' - L') and immunostained with anti-CLN1 (A, C, A', C', D, F, D' and F', green), anti-CLN5 (G, I, G', I', J, L, J' and L, green), anti-CI-MPR (B, E, H and K, red) or anti-myc following sortilin-myc transfection (B', E', H' and K', red). Arrows indicate the perinuclear staining of CI-MPR (B, E and H) and sortilin (B', E' and H') while stars indicate lack of perinuclear staining for CI-MPR (K) and sortilin-myc (K'). Scale bar = 10µm. (M) HeLa cells were transfected with HA-CLN5 following siRNA treatment (siCLN5 or siCLN1) as indicated. Whole cell lysates were Western blotted (Wb) with anti-HA, anti-CLN1 or anti-actin antibodies. HeLa cells were either mock- (N and O) or CLN5-depleted (P and Q) and immunostained with anti-CLN5 antibody (N - Q, green) and giantin (N and O, red) or TGN46 (P and Q, red). Arrows indicate the normal staining pattern of giantin and TGN46 while stars represent dispersed staining. Scale bar = 10µm.

Figure 3. CI-MPR and sortilin are degraded in CLN5-depleted cells. (A) HeLa cells transfected with sortilin-myc were mock-, CLN5- or CLN1-depleted and incubated with 50µg/ml cycloheximide for the times indicated. Total cell lysates were Western blotted (Wb) with anti-CI-MPR, anti-myc, anti-CD63 or anti-actin antibodies. (B) Quantification of 3 separate cycloheximide chase experiments for mock-, CLN1- or CLN5-depleted cells and Western blotted for endogenous anti-CI-MPR, anti-myc or anti-CD63 antibodies. (C) Total cell lysates from Hela cells that were mock- or CLN5-depleted were Western blotted with anti-cathepsin D or anti-actin antibodies.

Figure 4. Recruitment of the Vps26 subunit of retromer to endosomes requires CLN5. HeLa cells were mock- (A - C and G - I), CLN5- (D - F) or CLN1-depleted (J - L) and immunostained with anti-CLN5 (A, C, D, F, green), anti-CLN1 (G, I, J and L, green) and anti-Vps26 (B, C, E, F, H, I, K and L, red) antibodies. Arrows represent normal staining for CLN5, CLN1 and Vps26 while stars highlight lack of staining of CLN5 (D), CLN1 (J) and Vps26 (E)

staining. Scale bar = 10µm. (M) Representative image of Vps26-positive structures identified (red circles) by our *ad hoc* algorithm to determine the intensity of Vps26 staining in HeLa cells.

Figure 5. CLN5 is required to recruit retromer to endosomal membranes. (A) Quantification of the relative fluorescence intensity of Vps26 staining in mock- (white bar), CLN5- (black bar) or CLN1-depleted cells (gray bar). Bar graphs represent the relative intensity of Vps26 in (1400, 1300 and 3000) endosomes per condition respectively with error bars representing +/- SEM. (B) HeLa lysates from mock-, CLN1- and CLN5-depleted cells were run on a 12% polyacrylamide gel and Western blotted (Wb) with anti-Vps26 and anti-actin antibodies. (C) Quantification of the relative fluorescence intensity of CD63 staining in mock- (white bar) and CLN5-depleted (black bar) cells. Graph represents the quantification of the relative intensity of CD63 from 4800 and 4000 endosomes respectively with the error bars representing +/- SEM. (D) Quantification of the relative fluorescence intensity of SNX1 staining in mock- (white bar) and CLN5-depleted (black bar) cells. Graph represents the quantification of the relative intensity of SNX1 from 4000 and 2500 endosomes respectively with the error bars representing +/- SEM.

Figure 6. The cytosolic and membrane distribution of Vps26 and Vps35 are altered in CLN5-depleetd cells. (A) Cytosolic (C) and membrane (M) fractions from mock-, CLN5- or Rab7-depleted cells were stained with anti-Vps35, anti-Vps26, anti-SNX3, anti-SNX1, anti-AP3 and anti-Lamp2 antibodies. (F) Quantification of the cytosolic (white bars) and membrane fraction (black bars) of Vps26 and Vps35 from 3 separate experiments

Figure 7. Transient expression of wild-type HA-CLN5 rescues the recruitment of Vps26 in CLN5-depleted cells. (A) Hela cells were either mock- or CLN5-depleted with siRNA against the 3'UTR of CLN5. Cells were also transfected or not with HA-CLN5 and total cell lysates were Western blotted (Wb) for endogenous CLN5 using anti-CLN5, transfected HA-CLN5 with anti-HA antibody or anti-actin. (B) Quantification of the relative fluorescence intensity of Vps26 staining in mock- (white bar), CLN5-depleted cells (black bar) or CLN5-depleted cells transfected with HA-CLN5 (grey bars). Bar graphs represent the relative intensity of Vps26 in (3400, 2200 and 4700) endosomes per condition respectively with error bars representing +/- SEM.

Figure 8. CLN5 is required for the localization of Rab7. HeLa cells were mock- (A - C and G - I), CLN5- (D - F) or CLN1-depleted (J - L) and transfected with RFP-Rab7 (A - L). Following transfection, cells were fixed in 4% paraformaldehyde and then immunostained with anti-CLN5 (A, C, D and F, green) or anti-CLN1 (G, I, J and L, green) antibodies. Arrows indicate the normal distribution of CLN5 (A), CLN1 (G) and Rab7 (B, H and K). Stars indicate the lack of CLN5 expression (D) and the lack of recruitment of RFP-Rab7 (E) in CLN5-depleted cells. Scale bar = 10μm. (M) Quantification of the fluorescence intensity of RFP-Rab7 in mock- (white bar), CLN5- (black bar) and CLN1-depleted (gray bar) cells. Graph represent 5700, 9300 and 1600 endosomes per condition respectively with the +/- SEM. (N) Expression of RFP-Rab7 in mock- , CLN1- or CLN5-depleted cells was examined by Western blotting (Wb) with anti-RFP antibody. Anti-actin staining serves as a loading control. (O) Quantification of the fluorescence intensity of RFP-Rab5 in mock- (white bar) or CLN5-depleted (black bar) cells. Graph represents the quantification of 2800 and 4000 endosomes per condition respectively. (P) Expression of RFP-Rab5 in mock- and CLN5-depleted cells was examined by Western blotting (Wb) with anti-RFP antibody. Anti-actin staining serves as a loading control.

Figure 9. CLN5 is required for the activation of Rab7. (A) HeLa cells were transfected with HA-CLN5 and either myc-Rab1a, RFP-Rab5 or RFP-Rab7 as indicated. Total cell lysates were immunoprecipitated (IP) with anti-RFP or anti-HA antibodies and Western blotted (Wb) with either anti-HA, anti-myc or anti-RFP antibodies. The pre-immunoprecipitation (pre-IP) is shown and represents 10% of the input. (B) HeLa cells were co-transfected with HA-CLN5 and either wild-type RFP-Rab7, dominant active RFP-Rab7Q67L or dominant negative RFP-Rab7T22N. Total cell lysate was immunoprecipitated (IP) with anti-HA antibody and Western blotted (Wb) with either anti-RFP or anti-HA antibodies. The amount of RFP-Rab7, RFP-Rab7Q67L or RFP-Rab7T22N pre-immunoprecipitation (Pre-IP) is shown and represents 10% of the input. (C) The amount of GTP loaded Rab7 and Rab5 were determined using a non-hydrolysable biotin conjugated probe (Guanosine 5'-triphosphate [γ] 4-azidoanilide 2',3'-biotin-long chain-hydrazone) in mock or CLN5-depleted cells. The amount of loaded GTP probe was determined using streptavidin (stav) while the amounts of RFP-Rab7 or RFP-Rab5 were determined using anti-RFP antibody (Wb: RFP). (D) The relative intensity of GTP loaded Rab7 in mock- and CLN5-depleted cells from 3 independent experiments with the +/- SEM. (E) The relative intensity of GTP loaded Rab5 in mock- and CLN5-depleted cells from 3 independent

610 experiments with the +/- SEM. (F) GST-RILP$_{220-299}$ bound to glutathione-sepharose beads was
611 incubated with HeLa lysates expressing RFP-Rab7 that were either mock-, CLN1 or CLN5-
612 depleted. The amount of bound RFP-Rab7 was detected by Western blotting (Wb) with anti-RFP
613 antibody. The coomassie stained gel shows the amount of bound GST-RILP$_{220-299}$.
614 **Figure 10. Model showing the role of CLN5 in sorting from the endosomes.** When the cargo
615 loaded lysosomal sorting receptor (green line) arrives at the endosome (Step 1), the change in pH
616 causes a dissociation of the cargo form the receptor which that subsequently interact with CLN5
617 (Step 2). This the enables the recruitment and activation of Rab7 and the recruitment of retromer
618 (Step 3) to sort the back to the Golgi where it can interact with more cargo.

Mamo et al., Figure 1

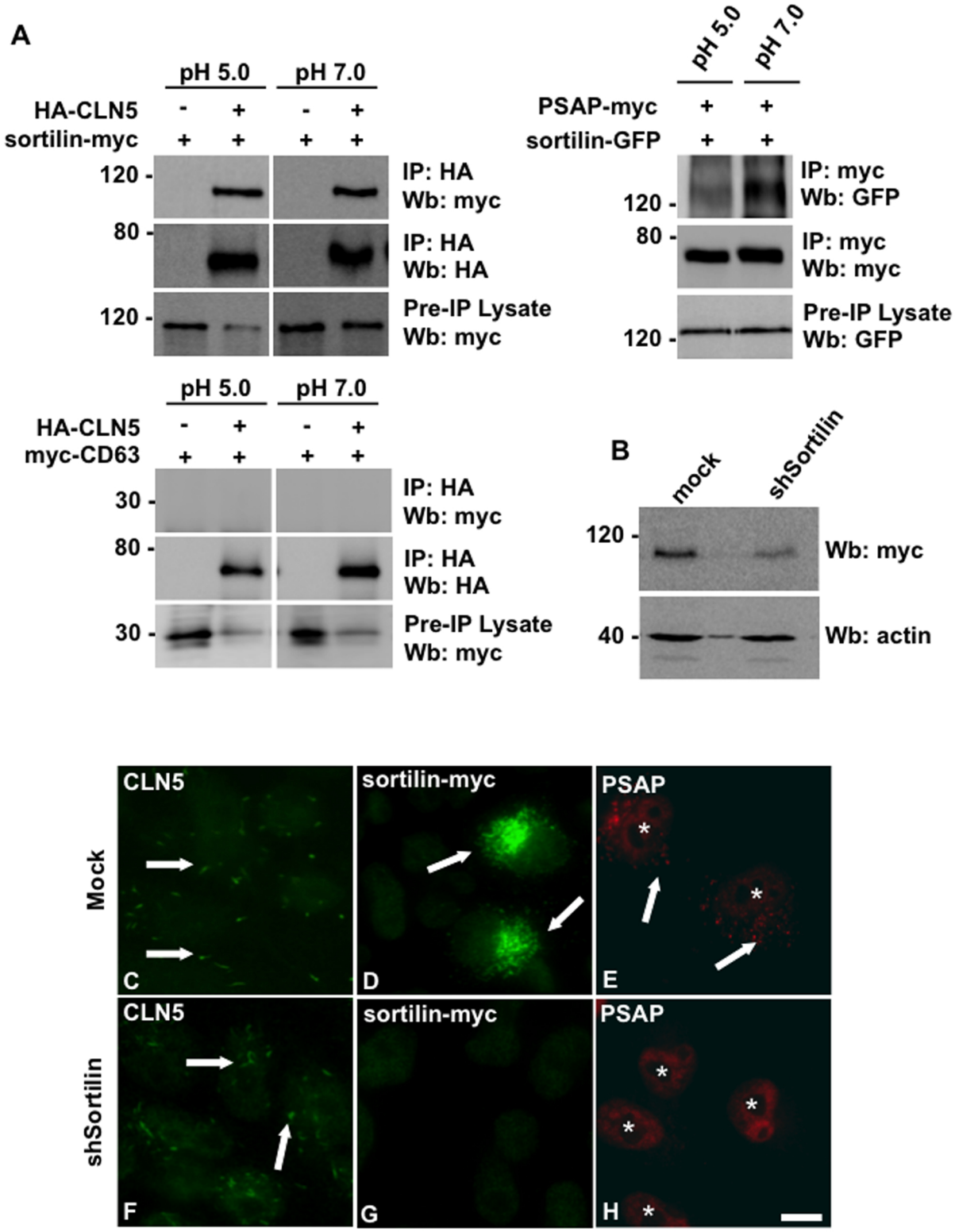

Mamo et al., Figure 2

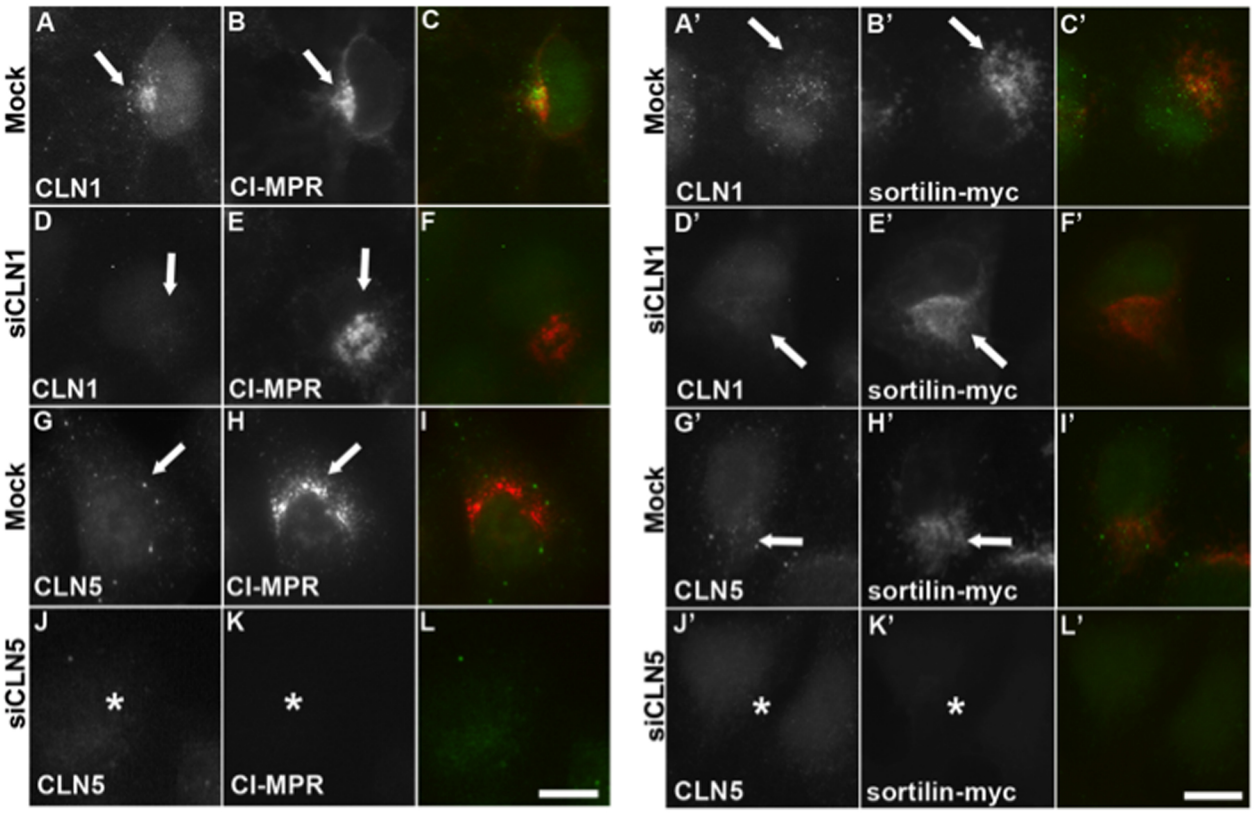

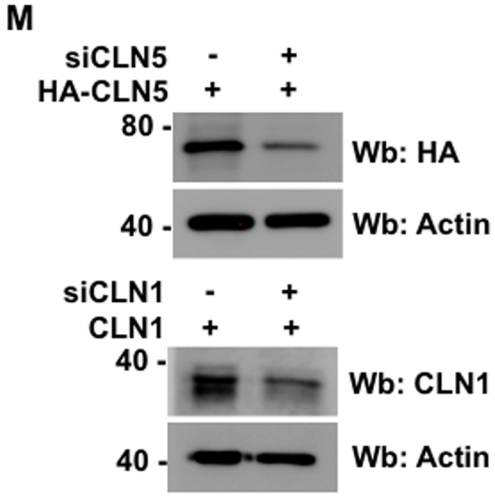

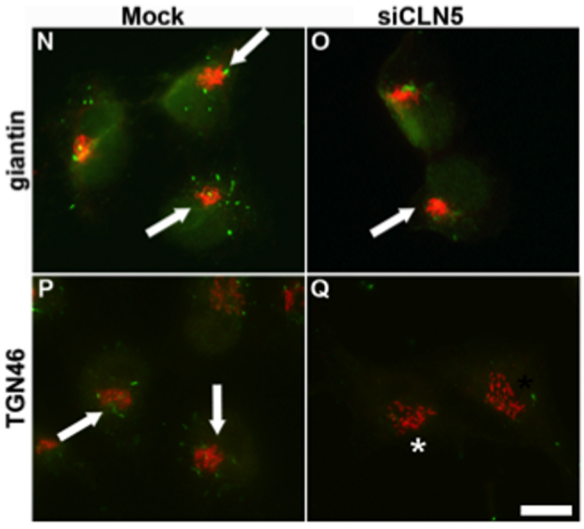

Mamo et al., Figure 3

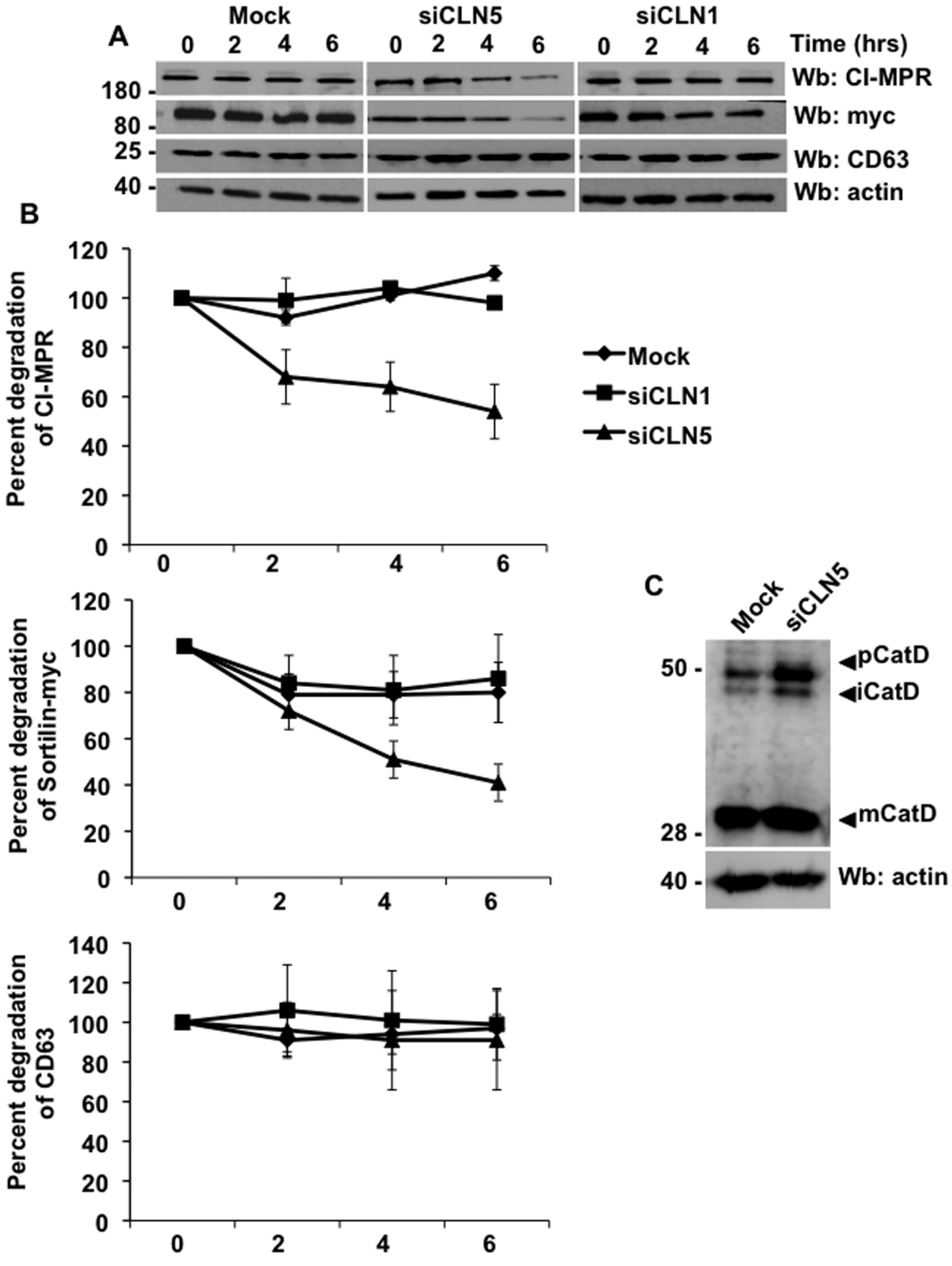

Mamo et al., Figure 4

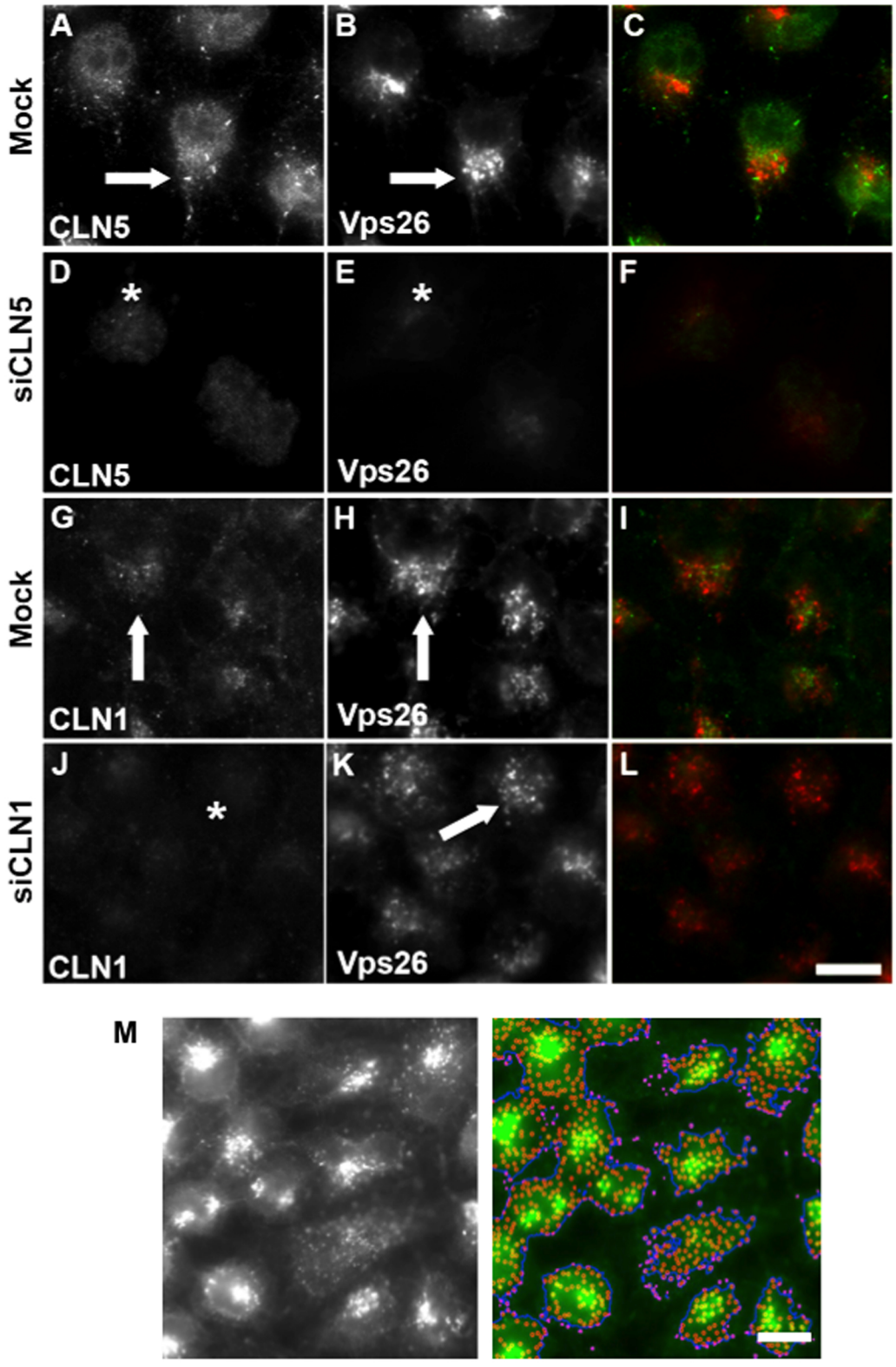

Mamo et al, Figure 5

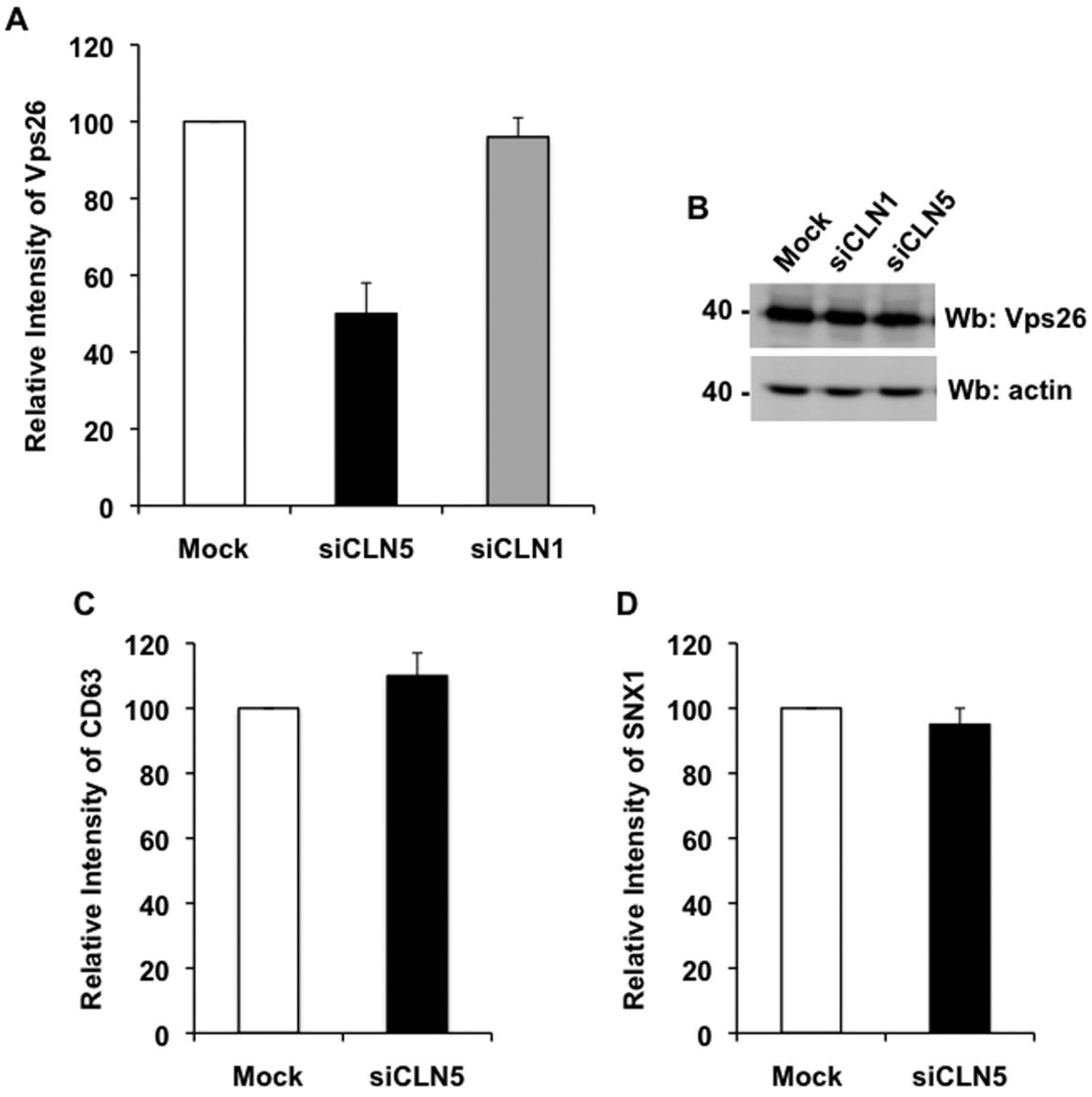

Mamo et al, Figure 6

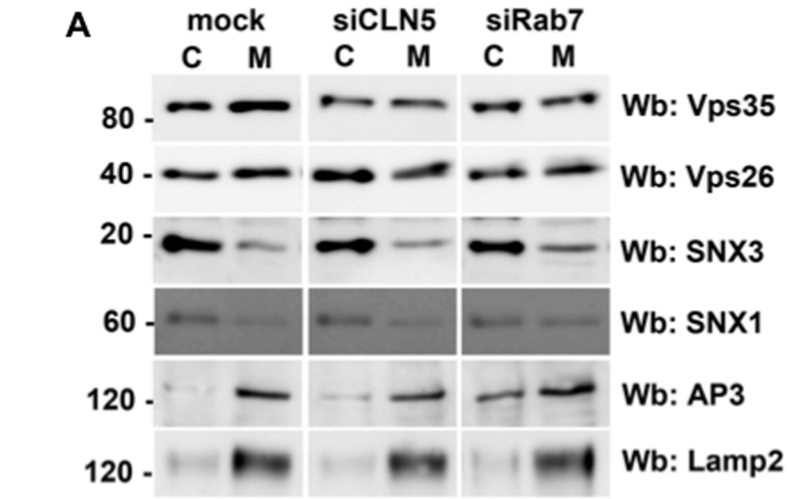

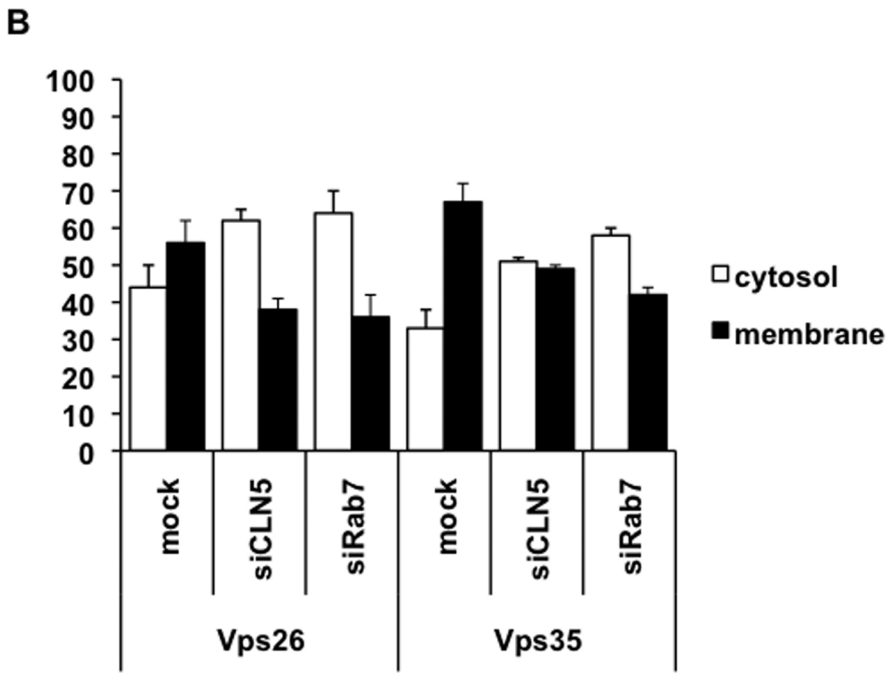

Mamo et al., Figure 7

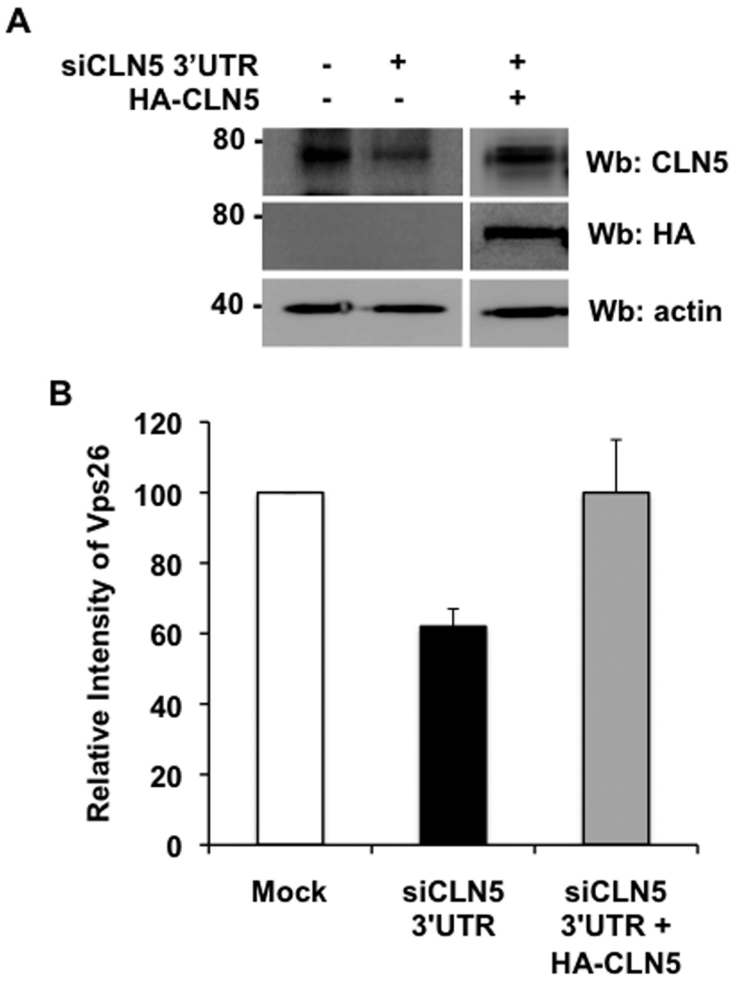

Mamo et al., Figure 8

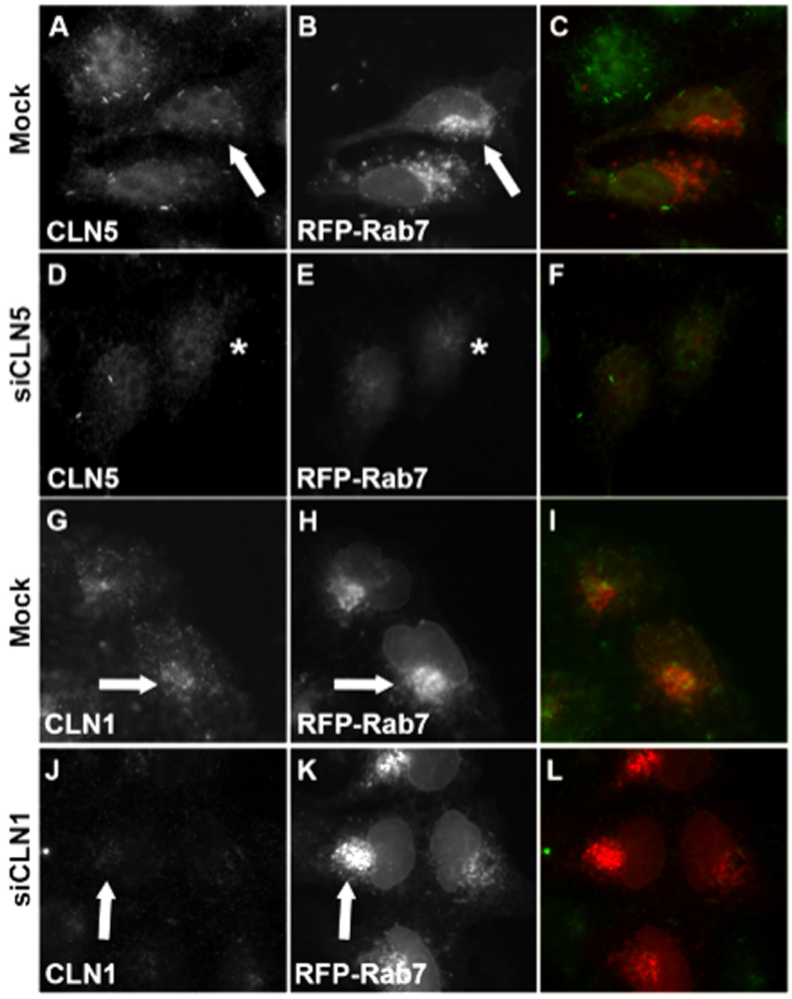

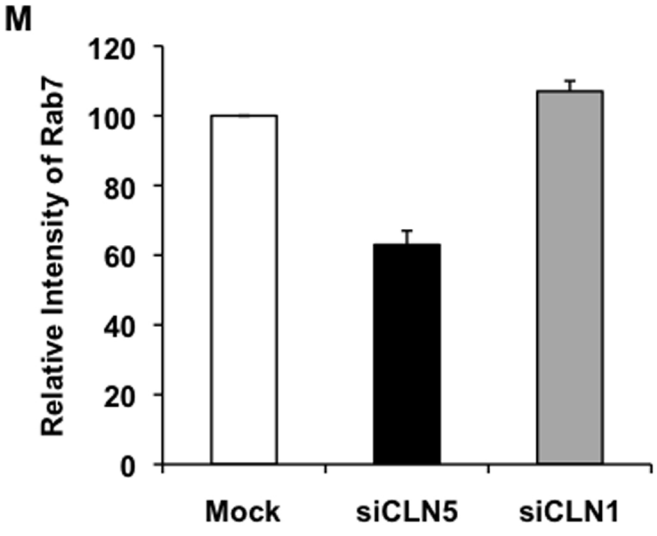

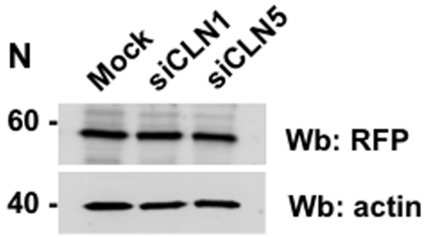

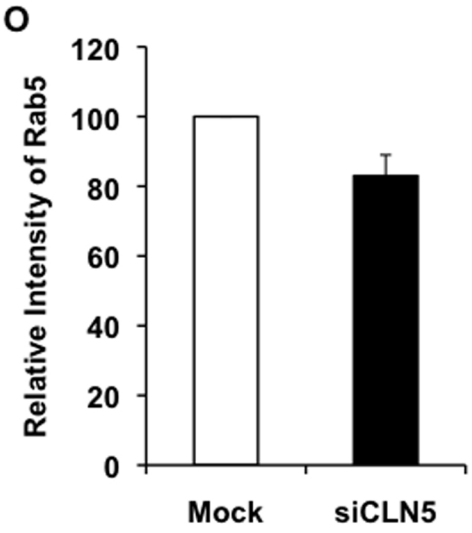

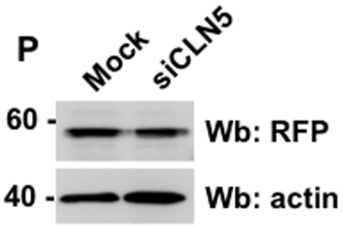

Mamo et al., Figure 9

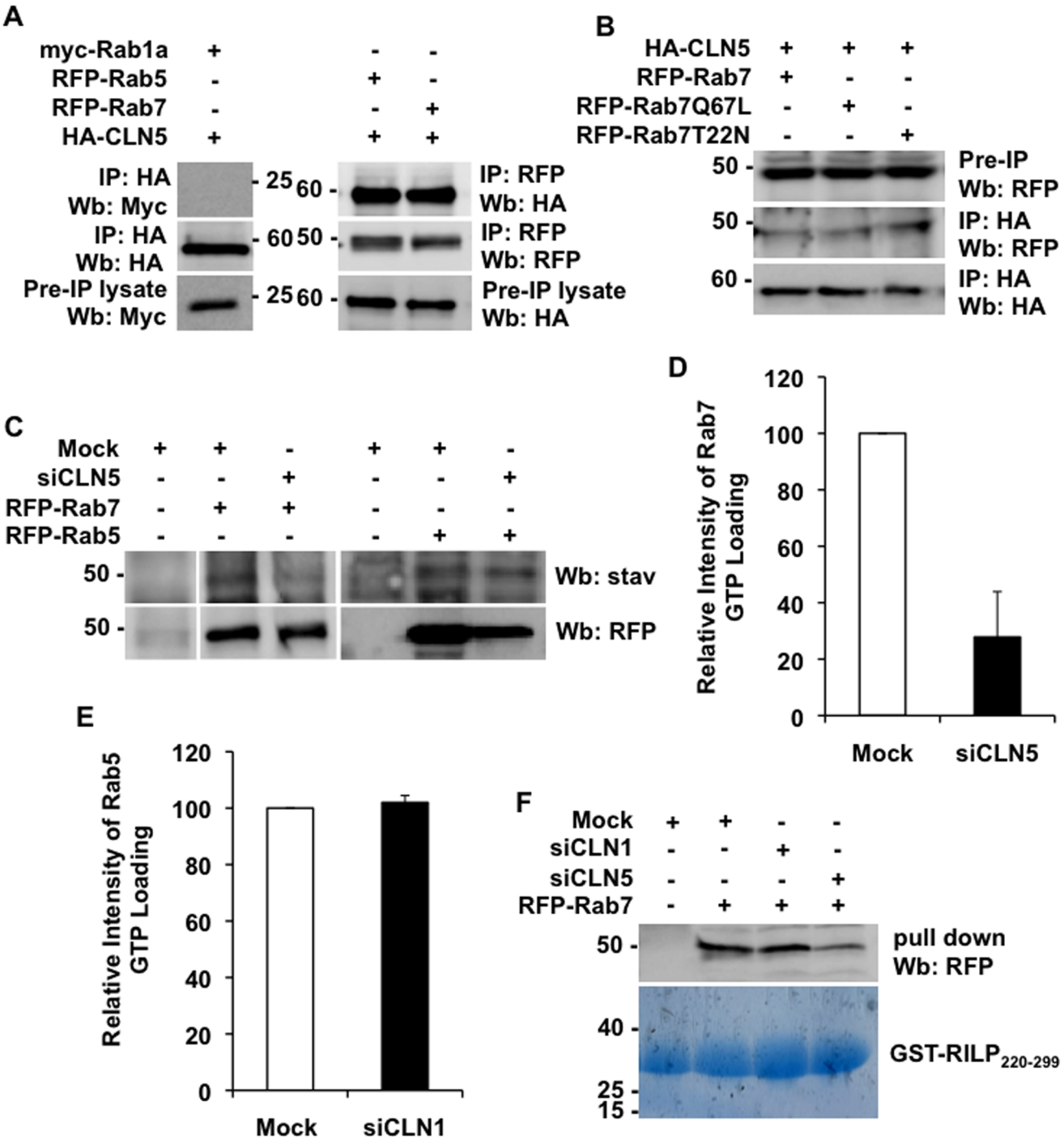

Mamo et al., Figure 10